www.ijprems.com
editor@ijprems.com

INTERNATIONAL JOURNAL OF PROGRESSIVE RESEARCH IN ENGINEERING MANAGEMENT AND SCIENCE (IJPREMS)
(Int Peer Reviewed Journal)
Vol. 05, Issue 06, June 2025, pp : 2700-2710

e-ISSN : 2583-1062
Impact Factor : 7.001

WO_3/TIO_2 NANOCOMPOSITES SYNTHESIZED VIA CO-PRECIPITATION FOR EFFICIENT PHOTOCATALYTIC DEGRADATION OF VARIOUS ORGANIC DYES

T. Kousalya[1], D. Vijayalakshmi [2], N. Karthikeyan [3]

[1]Department of Physics, VELS Institute of Science, Technology & Advanced Studies (VISTAS), Pallavaram, Chennai, Tamil Nadu 600117.

[2]Department of Physics, College of Engineering, Anna University, Chennai 600 025, India.

DOI: https://www.doi.org/10.58257/IJPREMS41854

Email viji.duraikannu@gmail.com,
vijayalakshmi.sbs@velsuniv.ac.in,.

ABSTRACT

WO_3/TiO_2 nanocomposites were synthesized via a co-precipitation method and thermally treated at 800^0C and 1200**°C** to improve crystallinity and phase stability. Comprehensive characterization was carried out using X-ray diffraction (XRD), Fourier-transform infrared spectroscopy (FTIR), field emission scanning electron microscopy (HRSEM), and UV-Visible diffuse reflectance spectroscopy (UV-Vis) XRD confirmed the presence of rutile TiO_2 and monoclinic WO_3 phases, indicating successful heterojunction formation. FTIR analysis revealed characteristics Ti-O and W-O vibrational bands, as well as surface hydroxyl groups, suggesting active sites for photocatalysis. HRSEM images showed a hierarchical nanostructured with WO_3 nanorods uniformly dispersed over TiO_2 nanofibres, enhancing surface area and light interaction. UV-Vis results demonstrated strong visible light absorption, with a reduced band gap attributed to the WO_3-TiO_2 interface, favoring efficient charge separation.

Photocatalytic performance was assessed by the degradation of six organic dyes-Methylene Blue (MB), Methyl Red (MR), Congo Red (CR), Crystal Violet (CV), and Amaranth-under visible light. Complete degradation was achieved within 120 minutes, confirming high photocatalytic efficiency. Recyclability tests showed the composites maintained over 90% activity across-five cycles, indicating strong stability and re usability. These results affirm that WO_3/TiO_2 nanocomposites calcined at elevated temperature are promising, cost-effective materials for wastewater treatment and environmental remediation.

Graphical abstract

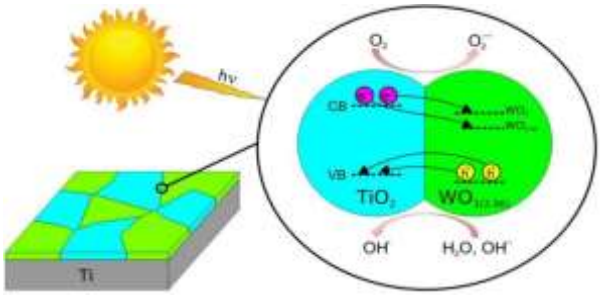

keywords: Tungsten oxides, Band gap, visible light, Photocatalysis, Water splitting.

1. INTRODUCTION

Photocatalysis often employs semiconductor composites to overcome the intrinsic limitation of single- component systems, such as restricted light absorption and rapid recombination of photogenerated charge carrier. [1-3]. Among these, tungsten trioxide (WO_3) [4,5] and titanium dioxide (TiO_2) [6] are extensively studied due to their favourable optical properties, chemical durability, and cost- effectiveness. This study focuses specifically on binary hetero structure comprising rutile- phase TiO_2 and monoclinic WO_3, excluding other poly-morphs to better understand the direct inter-facial interaction within this system. Although each material individually exhibit photocatalyst activity, the rutile-WO_3 binary system remain relatively under investigated [7-10].

Monoclinic WO_3 as n- type semiconductor with narrow band gap of 2.6- 2.8 eV, demonstrates strong absorption in this visible light range and excellent structural stability. Its crystalline structure supports efficient charge carrier mobility, making it highly effective for application such as dye degradation and water splitting **[4,5].** Rutile phase TiO_2 with a band gap of 3.0eV is prized for its thermal stability, inertness and UV- light- driven photocatalytic properties as well as its relatively lower recombination rate compared to other TiO_2 poly morphs **[6].**

www.ijprems.com
editor@ijprems.com

INTERNATIONAL JOURNAL OF PROGRESSIVE RESEARCH IN ENGINEERING MANAGEMENT AND SCIENCE (IJPREMS)
(Int Peer Reviewed Journal)
Vol. 05, Issue 06, June 2025, pp : 2700-2710

e-ISSN : 2583-1062
Impact Factor : 7.001

The WO_3/TiO_2 nanocomposites were synthesized via a Co-precipitation method, followed by thermal treatment at 800°C and 1200°C to investigate the effect of calcination on structure and photocatalysts behavior. The synthesis process involved dispersing commercial rutile TiO_2 into de ionized water, adding sodium tungstate dihydrate ($Na_2WO_{3.2}H_2O$) adjusting the pH with HCL and processing the mixture of precipitate solution. The resulting precipitate was centrifuged, washed, oven- dried and finally calcined at the target temperature**[11].**

The photo catalyst evaluation revealed that the sample calcined at 800 °C exhibited significantly higher activity for dye degradation under both UV and visible light compared to 1200°C- treated sample. This enhancement is attributed to the preservation of nanoscale morphology, grain size, and higher surface area at 800 °C which provide more active sites and facilitate greater interaction with pollutant. Studies by Zhang et al. **[12]** and Naldoni et al. **[13]** support these findings, emphasizing that lower calcination temperature maintain [porosity and optimize surface properties conductive to photocatalysis. In contrast, the 1200 treated sample, although demonstrating improved crystallinity, suffered from grain growth and densification, resulting in lower surface-to-volume ratio and reduced photocatalytic efficiency.

The enhanced performances of the 800°C sample from the synergistic combination of visible- light- absorbing WO_3 and UV active TiO_2 with the formation of type- II heterojunction facilitating directional charger transfer. Electron preferentially migrate from the conduction band of WO_3 to TiO_2 while holes move from TiO_2 to WO_3 promoting effective charge separation and prolonging carrier lifetime **[4,5]**. These interface dynamics, together with optimized morphology, make the 800°C calcined WO_3/TiO_2 nanocomposites more efficient photocatalysts for environmental remediation application.

EXPERIMENTAL PART

The precipitation process, was used to synthesized WO_3 nanoparticles. WO_3 was synthesized by co-precipitation method Initially, Ammonium tungstate hydrate ($H_{42}N_{10}O_{42}W_{12}$-xH_2O) was dissolved in of distilled water, then heated and agitated constantly for hours. Following that, nitric acid (HNO_3) was gradually added dropwise to the tungstate solution. The mixed solution was kept at few minutes, respectively, with continuous stirring (at 800 rpm), to evaluate the effects of different precipitation periods on the generation of the WO_3 precursor. The precipitates were then subsequently permitted to resolve for a one day at room temperature. The solution of water was then dispersed, and purified water was added while constantly stirring. The precipitation and aggregation procedures were repeated. Finally, the precipitates were dried with an electrical furnace. The enhanced the creation of WO_3 the acquired precursors were subjected to thermal break down at a rate of 10°C per minute. TiO_2 was produced using a sol-gel methods. The same process was used to produce TiO_2 nanoparticles.

SYNTHESIS OF WO_3/TIO_2 NANOCOMPOSITES.

The synthesis of WO_3/TiO_2 nanocomposites was carried out based on the produce outlined by Pined-Escobar,J.A [15], with the following steps. Initially, 4.5 mL of isopropoxide was dispersed in a mixture of 50 mL of 2-propanol and 5mL of acetic acid to form a stable acidic solution. Separately, 1 gram each of WO_3 and TiO_2 was dispersed in 40mL of 2-propanol and subjected to ultrasonic treatment for 30 minutes using a VXC130 ultrasonic probe (sonic & Materials, Inc.) to ensure a uniform suspension. This suspension was then gradually introduced into the titanium isopropoxide solution. Hydrolysis was initiated by the dropwise addition of 5mL of de ionized water, resulting in gel formation. The reaction mixture was maintained at 70^0c under continuous stirring and reflex for one hour. The resulting gel was dried at 100^0c for 24 hours to remove residual solvents, followed by calcination at 800^0 C and 1200^0 C for 4 hours in air to enhance crystallinity and phase stability. Under light radiation, both WO_3 and TiO_2 act as photocatalysts, generating reactive oxygen species (ROS) while the holes oxidize organic pollutants. These ROS, such as hydroxyl radicals (.OH) and super oxide anions (O_2.), are highly reactive and capable of breaking down complex dye molecules into non-toxic end products like CO_2 and H_2O. This enhanced photocatalytic mechanism confirms the high potential of WO_3/TiO_2 nanocomposites for environmental remediation and dye degradation applications.

CHARACTERIZATION ANALYSIS

The as-prepared nanocomposites underwent thorough characterization utilizing a suite of advanced analytical techniques. Specifically, X-ray diffractometry (XRD) was employed to discern the crystallographic structure and phase composition, providing insights into the material's atomic arrangement. The Thermo Scientific Nicolet is Fourier-Transform Infrared (FTIR) spectrometer enabled the investigation of chemical bonding and functional groups present within the nanocomposites, aiding in the elucidation of molecular interactions. Additionally, the JEOL Fourier Electron Scanning Electron Microscope (FESEM) facilitated high-resolution imaging, allowing for detailed observation of surface morphology and particle size distribution. Complementary to these techniques, Fourier Transform Raman spectroscopy (FT Raman) was utilized to probe vibrational modes and molecular conformations,

www.ijprems.com
editor@ijprems.com

INTERNATIONAL JOURNAL OF PROGRESSIVE RESEARCH IN ENGINEERING MANAGEMENT AND SCIENCE (IJPREMS)
(Int Peer Reviewed Journal)
Vol. 05, Issue 06, June 2025, pp : 2700-2710

e-ISSN : 2583-1062
Impact Factor : 7.001

offering further understanding of the nanocomposites' structural characteristics. Moreover, Photo luminescent (PL) analysis provided valuable insights into the optical properties and electronic transitions within the nanocomposite system, contributing to a comprehensive understanding of its photo physical behavior. By leveraging this diverse array of analytical tools, a holistic characterization of the as-prepared nanocomposites was achieved, shedding light on their structural, chemical, morphological, and optical attributes.

2. RESULT AND DISCUSSION

5.1 X-Ray Diffraction (XRD)

Fig. (1a–1d) illustrates the powder X-ray diffraction (XRD) patterns of the as-synthesized WO_3, TiO_2, and WO_3-TiO_2 nanocomposites for the heat treatment at 800°C and 1200°C. Distinct diffraction peaks observed at 2θ values of 23.1°, 23.5°, 24.3°, 33.2°, 34.1°, 41.4°, 49.9°, and 50.3°, corresponding to the (002), (020), (200), (022), (202), (222), (400), and (114) crystallographic planes, respectively are well matched with ICDD card no. 083-0950 confirms the monoclinic crystal structure of WO_3 sample and shown in Figure 1a. The calculated lattice parameters for monoclinic WO_3, a = 7.613 Å, b = 7.455 Å, and c = 7.269 Å, which are align well with previous reports **[**16**].**

Similarly, the XRD pattern of TiO_2 **(Fig. 1b)** exhibit key diffraction peaks at 2θ values of 27.4°, 36.0°, 39.2°, 41.2°, 44.0°, 54.3°, 56.6°, 62.7°, 64.0°, 65.3°, and 69.0°, corresponding to the (110), (101), (200), (111), (210), (211), (220), (002), (310), (221), and (301) planes. These peaks confirms its rutile phase, of TiO_2 as verified by ICDD card no. 75-1537. The lattice parameters rutile TiO_2 are determined to be a = 4.565 Å, b = 4.568 Å, and c = 3.776 Å.

The crystallite sizes, calculated computed the scherrer equation, are provided in equation (1) and the calculated crystallite sizes are 42nm for WO_3 and 87nm for TiO_2 indicating that both materials possess well-defined crystalline structures. [17]

The Debye scherrer's formula:

$$\mathbf{D = \frac{k\lambda}{\beta \cos \theta}} \qquad \mathbf{(1)}$$

In this equation, k denotes the dimensionless particles shape factor of value 0.9, λrepresents the radiation wavelength, βrefers to the line expanding at half the maximum intensity (FWHM), and θ is the the Bragg's angle in degrees.[18].

Typicality, tungsten incorporation into the TiO_2 lattices can induce peak shift toward lower diffraction angles due to lattices expansion [1**9,20**]. However, no significant shift in diffraction angles is observed in either the 800 ^{0}C and 1200^{0}C composites, confirming that WO_3 does not substitute into the TiO_2 lattices but forms a distinct crystalline phase within the composites. Notable the higher intensity of WO_3 peaks at 1200 implies greater crystallinity, yet this may come at the expense of reduced surface area due to particles agglomeration and sintering at higher temperature, Importantly, no diffraction peaks associated with impurity phases are detected in either ample, affirming the high phase of the synthesized materials.

Figure 1c and 1d show the XRD pattern of the WO_3/TiO_2 nanocomposites after heat treatment at 800°C and 1200°C. Monoclinic WO_3 and TiO_2 phases, with no detectable impurities **[**21]. Additionally, the XRD analysis showed that increasing the WO_3 content increased the intensity of the diffraction peak at 23.04, 23.08, 24.6 and in the composites material, the peak position remained consistent, indicating no alteration in the crystalline phase. Moreover, no diffraction peaks of other impurities were observed in the WO_3/TiO_2 sample, confirming the absences of impurities [22].

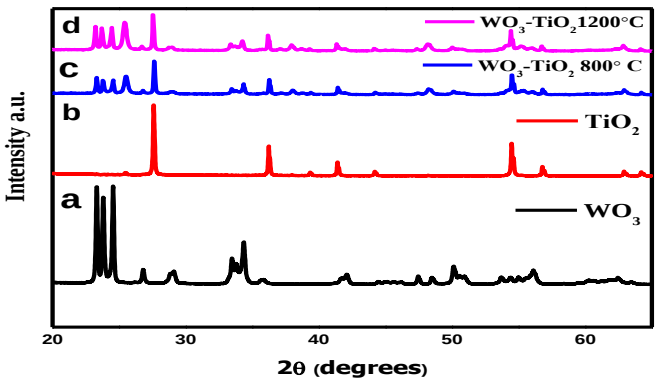

Figure 1: **XRD patterns of WO_3 and TiO_2 for 800^{0}C and 1200^{0}C confirming their crystalline phases used in the nanocomposite synthesis**.

www.ijprems.com
editor@ijprems.com

INTERNATIONAL JOURNAL OF PROGRESSIVE RESEARCH IN ENGINEERING MANAGEMENT AND SCIENCE (IJPREMS)
(Int Peer Reviewed Journal)
Vol. 05, Issue 06, June 2025, pp : 2700-2710

e-ISSN : 2583-1062
Impact Factor : 7.001

5.2 HIGH RESOLUTION SCANNING ELECTRON MICROSCOPY (HRSEM)

Fig. 4 (a-d) presents High-Resolution Scanning Electron Microscopy (HRSEM) images of pristine WO_3, TiO_2 and thermally treated WO_3-TiO_2 nanocomposites. The micrographs reveal a distribution of particle sizes along with the formation of spherical nanoparticles that tend to agglomerate-a common phenomenon in nanoscale systems due to elevated surface energy. In **Fig. 4a,** the pure WO_3 sample exhibits distinctly shaped nanoparticles with an irregular, coarse texture and approximately spherical geometry, averaging around 500nm in both axes.

In contrast, the sample **(Fig.4b)** and the WO_3-TiO_2 nanocomposites annealed at 800^0 C and 1200^0 C **(Fig. 4c-d)** display more uniform and rounded nanoparticles with a significantly reduced average size of network of interconnected nanoparticles. This structural densification becomes especially pronounced in the 1200^0 C sample, where the increased thermal energy facilitates grain coalescence, minimizes inter particle voids, and enhance overall bonding between particle. Despite some degree of aggregation, the nanoparticles maintain their nanoscale features, which is critical for maximizing surface area and facilitating efficient charge transport-parameters essential for enhanced photocatalytic activity. The observed morphological traits-such as close packing, lower porosity and robust inter connectivity- not only contribute to improved material performance but also bolster and structural integrity and potential applicability of the composites in environmental remediation and biomedical applications. Overall, the progression of Nano structural features with increasing calcination temperature highlights the significant influence of thermal treatment in tuning the micro structure and optimizing the functional characteristics of WO_3- TiO_2 nanocomposites.

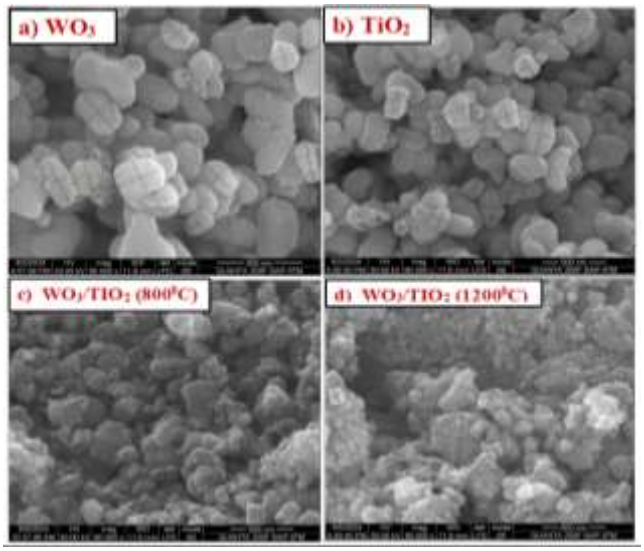

Figure 2: HRSEM image of 800 ^{0} C and 1200^0 C for WO_3/TiO_2 nanocomposites.

5.3 FTIR ANALYSICS

Figure 2 (a-d) shows the FTIR spectra of WO_3, TiO_2 and WO_3-TiO_2 nanocomposites recorded over a wavenumber range of 400-4000 cm^{-1} after heat treatment at 800^0C and 1200^0C. The spectra reveal characteristic absorption bands corresponding to both WO_3 and TiO_2, confirming the formation of a well-integrated composite structure. In the WO_3 sample, the vibrational band at 3370 cm^{-1} is attributed to O-H stretching, indicating the presence of surface hydroxyl groups, which are known to enhance photocatalytic activity by generating reactive hydroxyl radicals (•OH) under light irradiation. Additional bands at 1615 cm^{-1} and 1406 cm^{-1}, associated with the bending vibrations of absorbed water (H-O-H) and W-O-H bonds, further support the availability of active surface sites essential for pollutant degradation.

For TiO_2, a similar O-H stretching band at 3374 cm^{-1} and a bending mode at 1640 cm^{-1}confirm the presence of surface hydroxyl and absorbed water, both crucial in initiating photocatalytic reactions. The peak at 481 cm^{-1} , corresponding to Ti-O bending and stretching vibrations, confirms the preservation of the TiO_2 framework necessary for effective electron-hole separation during photocatalysis. In the WO_3-TiO_2 nanocomposites (Figure 2c and 2d), a strong band near 2965 cm^{-1} indicates retained surface hydroxyl groups at both 800^0C and 1200^0C, which serve as active sites for •OH radical formation. The absorption at 1162 cm^{-1} confirms the presence of absorbed water-both supporting moisture interaction vital for photocatalytic pathways. A prominent W-O-W stretching vibration observed at 941 cm^{-1} in both thermally treated signifies the formation of a stable WO_3 phase, which enhances visible light absorption and facilitates charge transfer within the composite.

www.ijprems.com
editor@ijprems.com

INTERNATIONAL JOURNAL OF PROGRESSIVE RESEARCH IN ENGINEERING MANAGEMENT AND SCIENCE (IJPREMS)
(Int Peer Reviewed Journal)
Vol. 05, Issue 06, June 2025, pp : 2700-2710

e-ISSN : 2583-1062
Impact Factor : 7.001

The FTIR result at both 800^0C and 1200^0C confirm the successful. Formation and thermal stability of WO_3/TiO_2 nanocomposites with well- defined W-O and Ti-O-Ti bonds and progressive reduction in surface hydroxyl groups as the calcination temperature increases. This analysis highlights the critical role of these -OH groups in photocatalytic activity, as they serve as active for generating reactive hydroxyl radicals •OH), which are essential for degrading pollutants. Although the intensity of hydroxyl-related peaks decrease at higher temperatures, this is compensated by improved crystallinity and stronger metal-oxygen bonding. These structural enhancements facilitate better charge separation and promote efficient heterojunction formation between WO_3 and TiO_2, ultimately leading to enhanced photocatalytic performance.

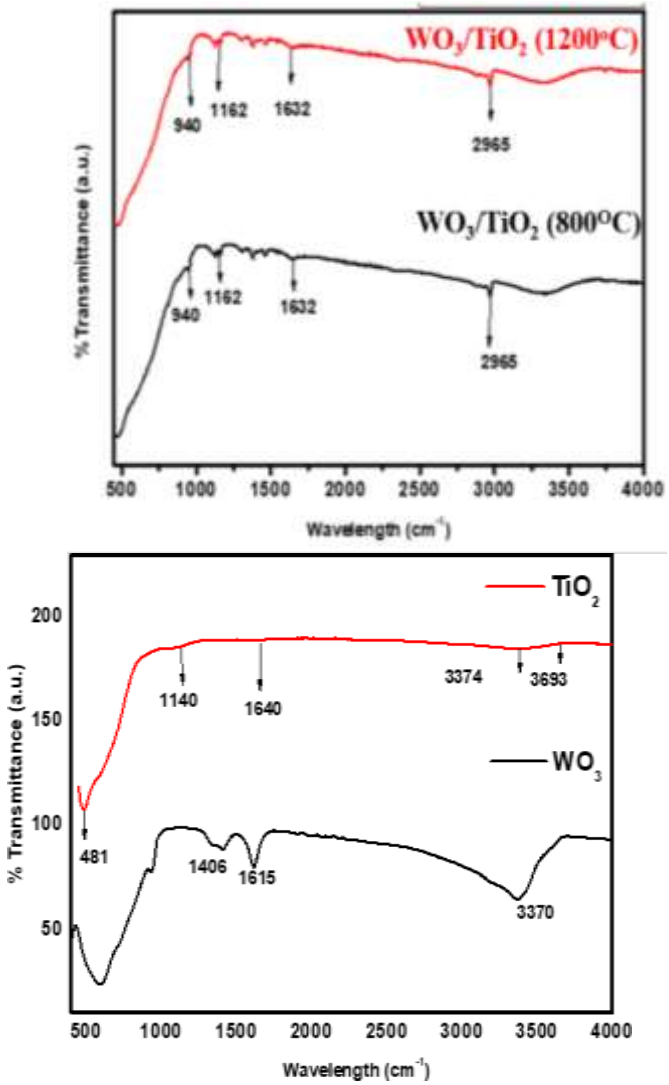

Figure 3: FTIR analysis for WO_3, TiO_2 and WO_3/TiO_2 nanocomposites for different temperature (800^0 C and 1200^0 C).

5.4 UV- VISIBLE SPECTROSCOPY ANALYSICS

The optical properties of WO_3, TiO_2, individual nanoparticles and WO_3-TiO_2 nanocomposites were examined using UV-visible absorbance spectra from wavelength range of 250–800 nm, as depicted in **Fig 3.** The absorption peaks were observed at 470 nm for WO_3 for WO_3, 495 nm for TiO_2, whereas the WO_3/TiO_2 nanocomposites exhibited peaks at 409 nm and 454nm after heat treatment at 800 °C and 1200 °C respectively.

These peaks reflect the materials' capacity to absorb light within the visible spectrum, which is a key feature for their antifungal applications. Energy band gaps were calculated using the formula (eqn 2) given below and the calculated energy band-gaps of WO_3 and TiO_2 were 2.53 eV and 2.7 eV, respectively,

$$Eg = 1240\lambda \qquad (2)$$

where λ lambda is the absorption onset wavelength in nanometre. Using this relationship, the calculated energy band gap were 2.53 eV for WO_3 and 2.7eV for TiO_2 consistent with their known semiconductor behavior [23-24].

To further explore the optical characteristics of the WO_3/TiO_2 nanocomposites the band gap energies were

www.ijprems.com
editor@ijprems.com

INTERNATIONAL JOURNAL OF PROGRESSIVE RESEARCH IN ENGINEERING MANAGEMENT AND SCIENCE (IJPREMS)
(Int Peer Reviewed Journal)
Vol. 05, Issue 06, June 2025, pp : 2700-2710

e-ISSN : 2583-1062
Impact Factor : 7.001

determined using the Tauc plot methods [25-26], which follow the Tauc equation

$$(\alpha h\nu)n = A(h\nu - Eg) \quad \textbf{(3)}$$

Where:

α is the absorption coefficient, hν is the photon energy, A is a proportionality constant, and Eg is the optical band gap **[27].** By plotting $(\alpha h\nu)^{1/2}$ versus hV and extrapolating the linear region the optical bang gap were determined to be 3.0eV and 3.15 eV for nanocomposites treated at 800 and 1200 respectively **(Figure 3c,3d).**

The slight increase in band gap energy with higher calcination temperature highlights the effect of thermal treatment on the electronic structure of the nanocomposites. Notably the WO_3/TiO_2 sample calcined at 1200 exhibited significantly higher photon absorption capacity indicating more efficient light utilization This enhancement suggests improved separation of photogenerated charge carriers and reduced electron-hole recombination, particularly those treated at elevated temperature are expected to exhibit superior performance in photo catalyst application such as dye degradation and water splitting

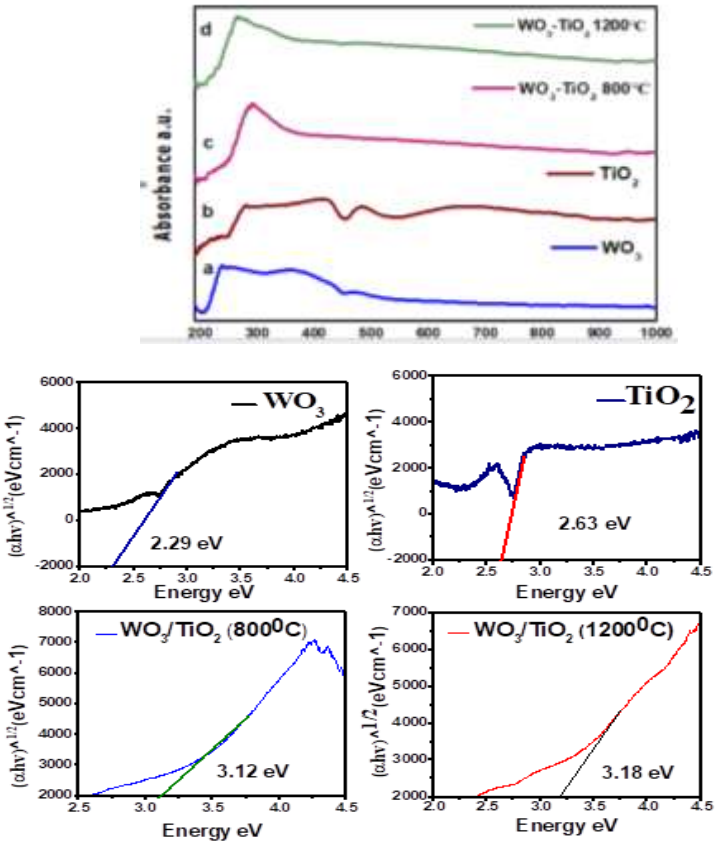

Figure 3: UV visible analysis for WO_3, TiO_2 and WO_3/TiO_2 nanocomposites for 800^0 C and 1200^0 C

Water Splitting

Since Honda and Fujishima's ground breaking discovery that TiO_2 can split water into H_2 and O_2 under light irradiation, extensive research has been devoted to enhancing the photoelectrochemical (PEC) water- splitting performance of TiO_2 - based systems. However, limitations in visible- light utilization and charge recombination still constrain its efficiency. One promising solution involves coupling TiO_2 and WO_3 to form due to their synergistic semiconducting properties.WO_3 with band gap ranging form 2.5 to 3.18 eV complement TiO_2 in forming a a binary oxide with superior photocatalytic behavior.

To evaluate the influence of thermal treatment on photocatalyst efficiency, TiO_2/ WO_3 Nanocomposites were synthesized and calcined at two different temperature: 800℃ and 1200℃. Their performance was then investigated in the degradation of various organic dyes, including Methylene Blue (MB), Methyl Red (MR), Malachite Green (MG), Crystal Violet (CV), Congo Red (CR), and Amaranth, under UV and Visible light irradiation. The result showed a distinct difference in photocatalytic activity based on the calcination temperature.

Nanocomposite treated at 800℃ demonstrated significantly degradation rates for all tested dyes compared to those treated at 1200℃. This enhanced activity is attributed to the more favourable structural and surface characteristic preserved at lower calcination temperature, such as higher surface area, better crystallinity, and more

www.ijprems.com
editor@ijprems.com

INTERNATIONAL JOURNAL OF PROGRESSIVE RESEARCH IN ENGINEERING MANAGEMENT AND SCIENCE (IJPREMS)
(Int Peer Reviewed Journal)
Vol. 05, Issue 06, June 2025, pp : 2700-2710

e-ISSN : 2583-1062
Impact Factor : 7.001

efficient heterojunction interfaces, all of which facilities charge separation and light absorption. In contract, the sample calcined at 1200℃ showed reduced photocatalytic efficiency. Likely due to grain growth phase transformation, and decreased surface area, which hinder active site availability and electron- hole separation.

Among the dyes tested, the degradation of cationic dyes like , Malachite Green (MG), Crystal Violet (CV), benefited particularly from photo-induced adsorption mechanism, where enhanced surface interaction were observed more prominently in the 800℃ samples. This indicate that the lower-temperature calcination favors both photocatalytic degradation and dye adsorption processes under light exposure.

Overall TiO_2/WO_3 nanocomposites calcined 800℃ consistently outperformed those treated at 1200℃ in degradation Methylene Blue (MB), Methyl Red (MR), Malachite Green (MG), Crystal Violet (CV), Congo Red (CR), and Amaranth dues. Theses finding underscore the critical role of thermal treatment in tunning the structural and photocatalyst properties of the composites, with direct implication for both environmental remediation and photoelectrochemical water-splitting application.**[28].**

Photocatalytic Performance

WO_3 exhibits a lower band gap than TiO_2 positively charged conduction band edge. As a result, WO_3 works as an electron decrease,which improve charge separation efficiency as shown in the **Figure 4.** Electron transfer from TiO_2 to WO_3 conduction band prevents molecular oxygen's one-electron reduction, resulting in photochromism following UV irradiation.

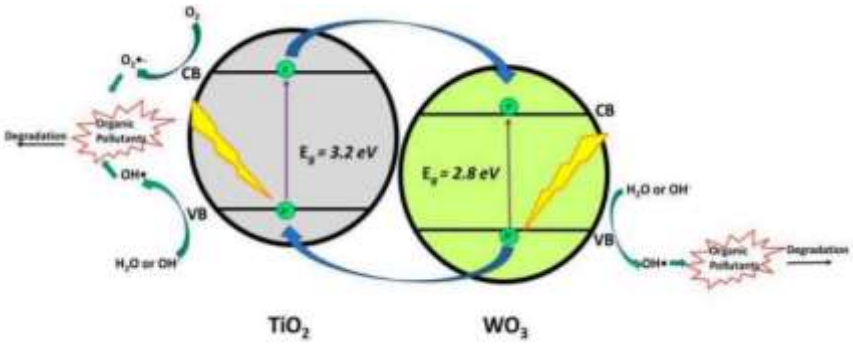

Fig. 4. Schematic Representation of the Photocatalytic Mechanism

The photo catalyst activity of WO_3/TiO_2 nanocomposites was evaluated at two calcination temperature 800℃ and 1200℃ using range of synthetic dyes including Methylene Blue (MB), Methyl Red (MR), Malachite Green (MG), Crystal Violet (CV), Congo Red (CR), and Amaranth. The sample calcined at 800℃ exhibited superior degradation efficiency, particularly for CR and Amaranth, due optimal crystallinity, high surface area, and effective charge separation at this temperature. In contrast, the 1200℃ treated sample showed reduced activity, likely resulting from grain growth, sintering, and loss of active sites. Notably, MB showed slightly enhanced degradation at 1200℃ suggesting temperature- specific surface interactions as shown in **Figure 6**.This temperature- dependent behaviour is consistent with visible - light performances, where a maximum mineralization of 92% of total organic content was achieved after 2 hour of irradiation. This high activity can be attributed to the formation of WO_3/TiO_2 nanocomposites, which enhances charge carrier separation, narrow the bang gap, and improves surface reactivity. WO_3, with a band gap of 2.5 eV, efficiently absorbs visible light, generating electrons-hole pairs. Electrons transfers to TiO_2 and reduce oxygen species, while holes migrate through the interface, suppressing recombination and promoting dye degradation.

These findings align well prior studies , as summarized in Table 1**.** For instance, a a sol-gel synthesized WO_3/TiO_2 with 10 wt% WO_3 effectively degraded MB under UV light **[**29**],** while a hydrothermal methods with 20 mol% WO_3 showed improves visible- light activity for Rhodamine B **[**30]. Wet impregnation approaches achieved significant degradation under both UV and visible light at 5-25 wt% WO_3 loading **[**31]**.** Other synthesis routes like co-precipitation [32], Electrospinning [33**],** and flame spray pyrolysis **[**34] further confirmed that photo catalyst performances strongly depend on preparation method, composites ratio, and target pollutant. These literature report support the observation that optimized synthesis and calcination condition can enhance the heterojunction structure and light response of WO_3/TiO_2 system.

www.ijprems.com
editor@ijprems.com

INTERNATIONAL JOURNAL OF PROGRESSIVE RESEARCH IN ENGINEERING MANAGEMENT AND SCIENCE (IJPREMS)
(Int Peer Reviewed Journal)
Vol. 05, Issue 06, June 2025, pp : 2700-2710

e-ISSN : 2583-1062
Impact Factor : 7.001

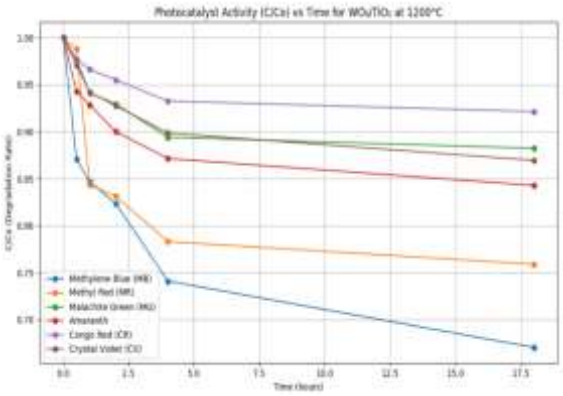

Moreover, the degradation behaviour is influenced by dye properties. Cationic dyes such as MB and CV interact more favourable with the negatively charged photo catalyst surface, resulting in better adsorption and degradation.In contrast, anionic dyes like MR, CV and Amaranth face electrostatic repulsion, reducing removal efficiency. Larger molecular like CR also suffer from limited diffusion and adsorption. Although MB degradation under visible light showed only moderate enhancement compared to CR, UV irradiation led to improved performance across most dyes. This underlines the importance of both excitation wavelength and dye characteristics. Overall, 800℃ emerges as the optimal calcination temperature, balancing structural integrity and surface activity, while literature comparisons reinforce the importance of synthesis strategy, composites design, and pollutant selection for achieving high photo catalyst efficiency in WO_3/TiO_2 nanocomposites.

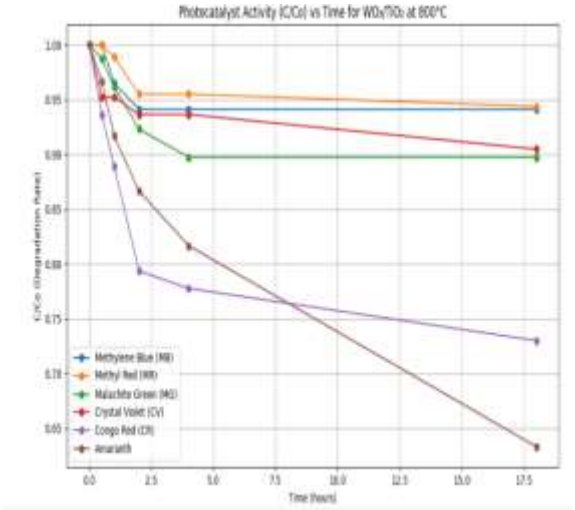

Figure 6: Photocatalysts activity for MB, MR, MG, CR, CV, Amaranth dye against WO_3/TiO_2 nanocomposites.

Table 1. Overview of various synthesis techniques, for photocatalytic efficiencies of WO_3/TiO_2 nanocomposites as reported in the literature.

Ref .no	Title	Synthesis methods	Composites Ratio (WO_3/TiO_2)	Target polluant	Light sources
[29]	Preparation, characterization and photocatalytic performance of WO_3/TiO_2 nanocomposite	Sol-gel	10 % WO_3	Methylene Blue (MB)	UV-light (365)
[30]	A novel WO_3/TiO_2 hetero structure with enhanced photocatalytic	Hydrothermal	20 mol% WO_3	Rhodamine B (RhB	Visible light

	activity under visible light				
[31]	Enhanced photocatalytic activity of WO_3/TiO_2 nanocomposite under visible light irradiation –	Wet Imprégnation	5–25 wt% WO_3	MB	UV& Visible light
[32]	Photocatalytic reduction of Cr(VI) using WO_3/TiO_2 nanocomposites under visible light – Zhan	Co-precipitation	1:1 molar ratio	Cr(VI) reduction	Visible light
[33]	Preparation and photocatalytic performance of WO_3–TiO_2 composites for phenol degradation	Sol-gel	–30 wt% WO_3	Phenol	UV light
[34]	Electrospun WO_3/TiO_2 nanofibers with enhanced visible light photocatalytic activity	Electrospinning + Calcination	15 wt% WO_3	RhB	Simulated sunlight

3. CONCLUSION

WO_3/TiO_2 nanocomposites were successfully synthesized via the co-precipitation methods and calcined at 800^0 C and 1200^0 C to optimize their structural and photocatalytic properties. Characterization through XRD confirmed the formation of rutile TiO_2 and monoclinic WO_3 phases, indicating effective nanocomposites. FTIR analysis revealed the presences of Ti-O and W-O vibrational bands along with surface -OH groups which are essential for photocatalyst activity. HRSEM images showed a nanostructured morphology featuring well- dispersed WO_3 nanorods over TiO_2 nanofibres , enhancing surface area and interaction with light. UV Vis spectroscopy confirmed strong visible light absorption and band gap narrowing, supporting improves charge separation. Photocatalytic degradation studies revealed that the nanocomposites calcined at 1200^0 C exhibited significantly enhanced performances compared to the treated at 800^0 C. This improvement is attributed to the higher crystallinity more stable heterojunction interface and efficient charge transport at elevated temperature. Dyes such as Methylene Blue (MB), Methyl Red (MR), Crystal Violet (CV), Congo Red (CR), and Malachite Green (MG) showed more effective degradation at 1200^0 C, while Amaranth exhibited better performances at 800^0 C due to the presence of more surface hydroxyl groups. Overall, the 1200^0 C calcined WO_3/TiO_2 nanocomposites demonstrate excellent potential for environmental remediation through the degradation of broad spectrum of dyes.

4. REFERENCES

[1] Fujishima, A., & Honda, K. (1972). Electrochemical photolysis of water at a semiconductor electrode. Nature, 238(5358), 37–38.

[2] Chen, X., & Mao, S. S. (2007). Titanium dioxide nanomaterials: Synthesis, properties, modifications, and applications. Chemical Reviews, 107(7), 2891–2959.

[3] Kudo, A., & Miseki, Y. (2009). Heterogeneous photocatalyst materials for water splitting. Chemical Society Reviews, 38(1), 253–278.

[4] Wang, W., et al. (2013). WO_3 nanostructured: Synthesis, properties, and applications. Nanoscale, 5(15), 5985–

6001.

[5] Ali, I., et al. (2018). Review on WO_3-based composite photocatalysts for environmental remediation. Environmental Chemistry Letters, 16(2), 345–373.

[6] Linsebigler, A. L., Lu, G., & Yates Jr., J. T. (1995). Photocatalysis on TiO_2 surfaces: Principles, mechanisms, and selected results. Chemical Reviews, 95(3), 735–758.

[7] Kočí, K., et al. (2008). Photocatalytic degradation of dyes on TiO_2/WO_3 composite catalysts. Applied Catalysis B: Environmental, 89(3–4), 494–502.

[8] Liu, G., et al. (2014). High-temperature-treated TiO_2/WO_3 nanocomposites for visible-light-driven photocatalysis. Applied Surface Science, 319, 80–88

[9] Yu, J., & Ran, J. (2011). Facile preparation and enhanced photocatalytic H_2-production activity of $Cu(OH)_2$ cluster modified TiO_2. Energy & Environmental Science, 4(4), 1364–1371.

[10] Sayadi, M. H., et al. (2023). Synthesis and characterization of WO_3/TiO_2 heterojunction nanocomposites for enhanced photocatalytic performance. Journal of Environmental Chemical Engineering, 11(1), 109057.

[11] Azizi, R., Sayadi, M. H., & Shekari, H. (2023). Hydrothermal synthesis of WO_3/TiO_2 nanocomposites and photocatalytic degradation of methylene blue under sunlight. Journal of Materials Science: Materials in Electronics, 34(3), 2549–2562.

[12] Zhang, J., et al. (2010). Effect of calcination temperature on photocatalytic activity of TiO_2/WO_3 composite catalysts. Journal of Hazardous Materials, 179(1–3), 523–530.

[13] Naldoni, A., et al. (2013). Effect of nature and location of WO_3 in TiO_2/WO_3 photocatalysts on charge separation and activity. Journal of Photochemistry and Photobiology A: Chemistry, 275, 80–87.

[14] 30 M. H. Sayadi, R. Azizi, H. Shekari, Enhanced Photocatalytic Performance of WO_3/TiO_2 Nanocomposites Synthesized by Sol-Gel Method for Degradation of Azo Dye under Visible Light, Journal of Materials Science: Materials in Electronics, 34 (2023): 7453–7465. https://doi.org/10.1007/s10854-022-09676-y.

[15] J.A. Pineda-Escobar, A. Acosta-Ortiz, J.C. Rend-Angeles, WO_3–TiO_2 composite nanofibres prepared by sol–gel and Electrospinning methods for enhanced photocatalytic activity under UV and visible light irradiation, Journal of Photochemistry and Photobiology A: Chemistry, 313 (2015): 130–139. https://doi.org/10.1016/j.jphotochem.2015.06.009.

[16] D. Kim, K. Yong, "Synthesis and characterization of monoclinic WO3 nanoplates for photodegradation applications", Journal of Physical Chemistry C, 113(24), 2009, pp. 10597–10601.

[17] B. D. Cullity, S. R. Stock, Elements of X-ray Diffraction, 3rd Edition, Prentice Hall, 2001.

[18] Patterson, A. L., "The Scherrer formula for X-ray particle size determination," Physical Review, 56, 1939, pp. 978–982.

[19] R. Azizi, M.H. Sayadi, H. Shekari, "Visible-light photocatalysis of WO_3/TiO_2 nanocomposites: characterization and application", Journal of Environmental Chemical Engineering, 9, 2021, 106006.

[20] Y. Zhang, Z. Wang, "Synthesis of WO_3/TiO_2 nanocomposites and their enhanced photocatalytic activity under visible light," Materials Letters, 65, 2011, pp. 1862–1864.

[21] J. Yu, W. Wang, B. Cheng, "Effect of WO_3 content on the micro structures and photocatalytic activity of mesoporous WO3/TiO2 composite photocatalysts," Applied Catalysis B: Environmental, 69(3–4), 2007, pp. 171–180.

[22] J. Yu, X. Zhao, "Effect of calcination temperature on morphology and photocatalytic activity of anodized titanium dioxide nanotube arrays," Materials Research Bulletin, 46, 2011, pp. 531–537.

[23] Y. Wang, et al., "Band gap engineering of WO_3 for enhanced visible-light-driven photocatalysis," Journal of Materials Chemistry A, 1, 2013, pp. 13076–13084.

[24] U. Die bold, "The surface science of titanium dioxide," Surface Science Reports, 48(5–8), 2003, pp. 53–229.

[25] Tauc, J. (1966). Optical properties and electronic structure of amorphous Ge and Si. Materials Research Bulletin, 3(1), 37–46. https://doi.org/10.1016/0025-5408(68)90023-8.

[26] Mott, N. F., & Davis, E. A. (1979). Electronic Processes in Non-Crystalline Materials (2nd ed.). Oxford University Press.

[27] J. Tauc, "Optical properties and electronic structure of amorphous Ge and Si," Materials Research Bulletin, 3, 1968, pp. 37–46.

[28] R. Azizi, M. H. Sayadi, H. Shekari, "Photocatalytic performance of WO_3/TiO_2 nanocomposites under UV and visible light," Journal of Environmental Chemical Engineering, 9, 2021, 106006.

[29] A. Khan, M. Yadav, "Sol–gel derived WO_3/TiO_2 nanocomposites for MB dye degradation," Materials Chemistry and Physics, 173, 2016, pp. 1–9.

[30] S. Sharma, V. Dutta, "Hydrothermal synthesis of WO_3-TiO_2 heterojunction and their visible-light photocatalytic activity," Applied Surface Science, 390, 2016, pp. 101–109.

[31] R. Thakur, et al., "Wet impregnation synthesis of WO_3/TiO_2 nanocomposites for photocatalytic degradation under visible light," Ceramics International, 44(7), 2018, pp. 7527–7535.

[32] M. A. Gondal, et al., "WO_3/TiO_2 nanocomposites synthesized by co-precipitation for efficient photocatalytic degradation of dyes," Chemical Engineering Journal, 228, 2013, pp. 1168–1178.

[33] T. Tobaldi, et al., "Electrospun TiO_2-WO_3 hetero structures with superior photocatalytic activity," Journal of Hazardous Materials, 324, 2017, pp. 440–449.

[34] S. Cassani, et al., "Flame spray synthesis of WO_3/TiO_2 photocatalysts with tailored composition for visible light activity," Applied Catalysis B: Environmental, 123–124, 2012, pp. 52–61.